Antenna/Human Body Coupling in 5G Millimeter-Wave Bands: Do Age and Clothing Matter?

Giulia Sacco, Denys Nikolayev, Ronan Sauleau, Maxim Zhadobov

▶ **To cite this version:**

Giulia Sacco, Denys Nikolayev, Ronan Sauleau, Maxim Zhadobov. Antenna/Human Body Coupling in 5G Millimeter-Wave Bands: Do Age and Clothing Matter?. IEEE Journal of Microwaves, 2021, 1 (2), pp.593-600. 10.1109/JMW.2021.3063256 . hal-03376843

HAL Id: hal-03376843
https://hal.science/hal-03376843

Submitted on 18 Oct 2021

HAL is a multi-disciplinary open access archive for the deposit and dissemination of scientific research documents, whether they are published or not. The documents may come from teaching and research institutions in France or abroad, or from public or private research centers.

L'archive ouverte pluridisciplinaire **HAL**, est destinée au dépôt et à la diffusion de documents scientifiques de niveau recherche, publiés ou non, émanant des établissements d'enseignement et de recherche français ou étrangers, des laboratoires publics ou privés.

IEEE Journal of Microwaves

Received 24 January 2021; revised 19 February 2021; accepted 21 February 2021. Date of publication 2 April 2021; date of current version 7 April 2021.

Digital Object Identifier 10.1109/JMW.2021.3063256

Antenna/Human Body Coupling in 5G Millimeter-Wave Bands: Do Age and Clothing Matter?

GIULIA SACCO (Member, IEEE), DENYS NIKOLAYEV (Member, IEEE), RONAN SAULEAU (Fellow, IEEE), AND MAXIM ZHADOBOV (Senior Member, IEEE)

(Invited Paper)

CNRS, IETR (Institut d'Électronique et des Technologies du numéRique), UMR 6164, Univ Rennes, F-35000 Rennes, France

CORRESPONDING AUTHOR: Giulia Sacco (e-mail: giulia.sacco.it@gmail.com).

This work was supported by the French National Research Program for Environmental and Occupational Health of ANSES under Grant 2018/2 RF/07 through the NEAR 5G Project.

ABSTRACT With the fast development of 5th generation (5G) mobile networks and prominence of the personal area networks and human-centered communications, people of all ages are increasingly exposed in the upper part of the microwave spectrum. In some exposure scenarios, presence of a textile between the radiating source and skin can affect the power absorption. This study investigates, for the first time, the effect of ageing and impact of textile on the power deposition in a skin-equivalent model under near-field exposure induced by multi-beam radiating structures at 26 GHz and 60 GHz. An array of four Yagi antennas has been used as a representative example of 5G reconfigurable antennas. The maximum increase of the averaged absorbed power density with respect to the averaged value for adults is observed at 70 year (8.8% at 26 GHz and 6.9% at 60 GHz). The strongest decrease is for 5-years-old children (−4.5% at 26 GHz and -3.7% at 60 GHz). In presence of a textile, the absorbed power density can increase or decrease depending on the textile properties (thickness and permittivity) and on the thickness of the air gap between textile and skin. With cotton and wool (considered as representative textile materials) the maximum increase of the averaged absorbed power density is about 40% compared to the bare skin.

INDEX TERMS 5G, ageing, electromagnetic dosimetry, millimeter waves (MMW), textile.

I. INTRODUCTION

The increasing need for exchanging high amounts of data and more secured communications has resulted in the shift of operating frequencies towards millimeter waves (MMW) [1], [2]. At these frequencies, channel capacity is enhanced compared to sub-6 GHz bands, and larger bandwidths are available for high data rate communications.

Nowadays, with the wide spread of mobile devices, more and more children and seniors are exposed to radiofrequency radiation sources. At microwave frequencies, the difference in exposure levels between children and adults was investigated [3]–[5]. It was demonstrated that, up to 5.6 GHz, the whole-body-average specific absorption rate (SAR) in children can go beyond the exposure limits [6], [7] by 40%–45% whereas remaining below these limits for adults (given the same incident field) [5], [8]. A more recent study [9] investigated the whole-body average SAR using the child models specified by the Commission on Radiological Protection (ICRP) instead of the scaled adult phantoms. In this case, the SAR increase in children was of the same order of magnitude as the numerical calculation uncertainties. At MMW, the interaction between human tissues and antennas was discussed in [10]–[13]. Refs. [10], [11] mainly focused on the antenna performance rather than on the exposure assessment. In [12], [13], a dosimetric study in presence of a radiating device is described. The age effect on exposure at MMW was analyzed in [14] considering a plane wave as source. However, age-dependent variations of the absorbed power density have never been studied for MMW antennas.

This work is licensed under a Creative Commons Attribution 4.0 License. For more information, see https://creativecommons.org/licenses/by/4.0/

The exposure is typically assessed considering bare skin. In practice, several exposure scenarios involve the presence of textile interposed between a radiating source and skin (e.g., browsing when using gloves or making a phone call when wearing a hat). Under these conditions, the textile could act as a matching layer affecting the power absorption in the tissues [14]–[16]. The effect of clothing at MMW was previously investigated for a plane wave illumination. To the best of our knowledge, no data related to exposure to realistic sources in presence of textiles have been reported.

With the 5G of mobile networks new frequency ranges are explored. In Europe, the bands allocated for 5G are *n*257 (26.5–29.5 GHz), *n*258 (24.25–27.5 GHz), *n*260 (37–40 GHz), and *n*261 (27.5–28.35 GHz) [17]. The 60 GHz band (57–66 GHz in Europe [18]) is also identified as promising, in particular for small cells. This shift towards the upper part of the microwave spectrum impacts the antenna design for emerging wireless devices. Due to the elevated path losses at MMW, a high antenna gain is required. For this reason, directive multibeam phased arrays are increasingly used [19]–[30]. At these frequencies, end-fire antennas are usually preferred to broadside ones for user terminals [21], [27], [31], [32]. Indeed, if the antenna is positioned at the edge of a wireless device, the user shadowing affects less the antenna performance.

This study deals with the electromagnetic exposure under near-field conditions considering typical reconfigurable antennas at 26 GHz and 60 GHz. For the first time, the analysis is performed taking into account biological tissue permittivity variations with age and presence of a textile in proximity or in contact with skin. Since the power dissipation in the human body at 26 GHz is similar to the one in the lower part of the MMW band, in the rest of the paper we refer to this frequency as MMW for the sake of simplicity.

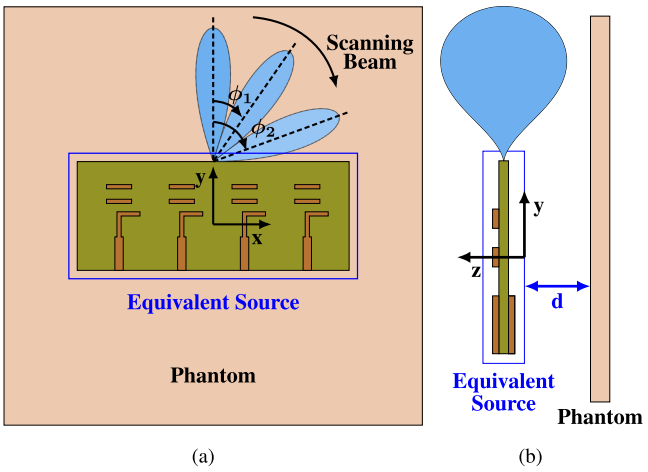

FIGURE 1. Exposure scenario: (a) front view and (b) lateral view. The dimensions are not to scale.

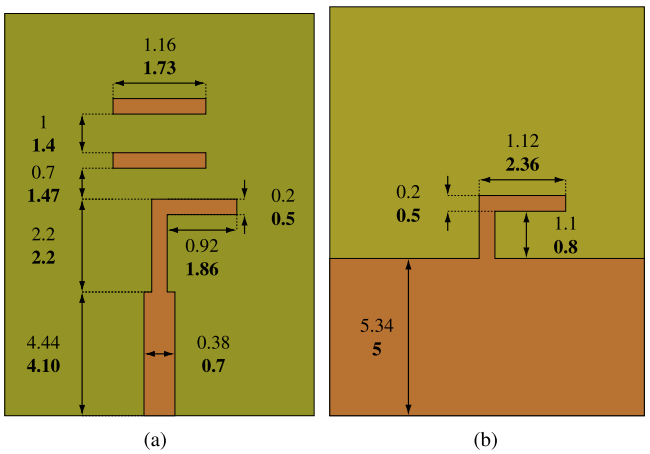

FIGURE 2. Yagi antenna geometry: (a) top and (b) bottom. The dimensions are in mm; those in bold refer to 26 GHz and the ones in regular font to 60 GHz.

II. MATERIALS AND METHODS

To simulate the exposure scenario of a phone call—i.e., when the phone is placed close to the head—the configuration represented in Fig. 1 was considered.

A. GENERIC MULTIBEAM ANTENNA

Two Yagi antennas with parallel polarization are considered as representative radiating structures at 26 GHz and 60 GHz. The design is inspired by recently reported antennas for 5G applications [22], [23]. The antenna topology and dimensions are reported in Fig. 2. Each radiating element is composed on the top layer by a driven element and two directors used to enhance the gain. The currents on the directors are induced by mutual coupling. These currents are almost equal in magnitude to the ones of the driven element but, according to the directors length and spacing, they introduce progressive phase shifts that reinforce the field in the directors direction. On the contrary, the truncated ground plane, acts as a reflector and impacts the front-to-back ratio without almost no modification of the antenna gain [33]. The antennas are designed on a Rogers RO4350B substrate ($\varepsilon_r = 3.48$, $\tan\delta = 0.0037$) [34] with a thickness of 0.508 mm at 26 GHz and of 0.254 mm at 60 GHz. The input reflection coefficients of these two antennas are represented in Fig. 3. An array of 4 elements at each frequency is considered to further increase the gain and allow for the reorientation of the main beam. The inter-element spacing equals 5.77 mm at 26 GHz and 2.34 mm at 60 GHz. By changing the phases at the ports of the array elements, the beamstearing performance can be evaluated. Fig. 4 shows the antenna gain for linear phase shifts α equal to 0° (beam pointing broadside), 50° (beam pointing at 15°), 100° (beam pointing at 30°), and 142.5° (beam pointing at 45°).

B. SKIN-EQUIVALENT MODEL

As at MMW the penetration depth is mainly limited to skin, the tissue model is represented by a homogeneous planar skin layer (Fig. 1; 6 cm × 6 cm × 2 mm at 26 GHz and 4 cm × 4 cm × 1mm at 60 GHz). For local near-field exposure, the planar approximation is justified by the fact that the typical radius of the body curvature exceeds by about five times

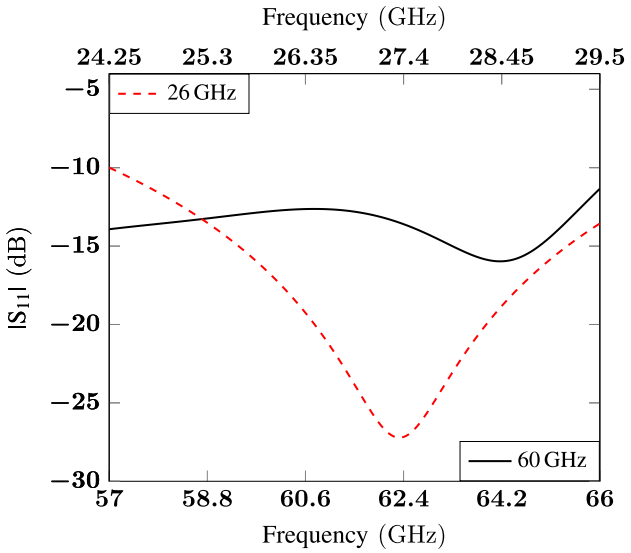

FIGURE 3. Reflection coefficients of 26 GHz and 60 GHz antennas.

the penetration depth at these frequencies avoiding the wave interference inside the body [35]. The typical permittivity of adult dry skin is $17.71 - j16.87$ at 26 GHz and $7.98 - j10.90$ at 60 GHz [36]. Age-dependent permittivity model was introduced in [14] and expresses the complex permittivity of tissues as a function of the TBW, representing the ratio between the amount of water in the human body and the person weight [37], [38]. The age-dependent complex permittivity is calculated as

$$\varepsilon^* = \varepsilon'_W{}^{\frac{\alpha-\alpha_A}{1-\alpha_A}} \varepsilon'_A{}^{\frac{1-\alpha}{1-\alpha_A}} \left(1 - j\frac{\varepsilon''_A}{\varepsilon'_A}\right), \tag{1}$$

where a ε'_W is the real part of the water permittivity [39], ε'_A and ε''_A are the real and imaginary parts of the adult skin permittivity [36], $\alpha(age) = TBW(age) \cdot \rho$ and $\alpha_A = TBW_A \cdot \rho$, where $TBW(age)$ and TBW_A are the TBW as a function of age and an average value for an adult [37], [38], respectively, and $\rho = 1109\ \mathrm{kg/m^3}$ is the skin density [40]. Cotton and wool have been considered as representative commonly used textiles. Their permittivity, measured at 60 GHz [41], is of $2 - j0.04$ for cotton and $1.22 - j0.036$ for wool. The permittivity of textile materials is assumed to be constant inside the frequency range considered in this study.

C. NUMERICAL MODELLING

The exposure scenario was simulated with the time-domain solver of CST Microwave Studio using the finite integration technique (FIT). Perfectly matched layers (PML) were used as exterior boundary conditions. The antenna was simulated separately and replaced by an equivalent source in the final model to speed-up the computation. The currents flowing on this equivalent source were computed in free space on the closed box surrounding the antenna ($27.33 \times 14.02 \times 2.93\ \mathrm{mm^3}$ at 26 GHz and $17.05 \times 12.36 \times 1.39\ \mathrm{mm^3}$ at 60 GHz). The equivalent source is then placed in proximity of the phantom

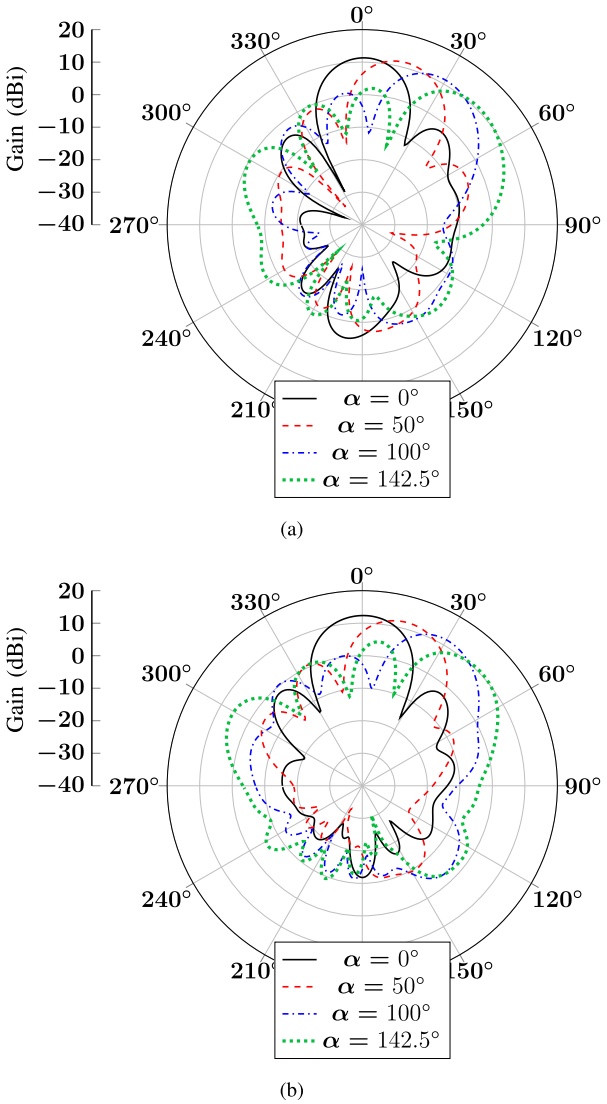

FIGURE 4. Radiation pattern (a) at 26 GHz and (b) 60 GHz for different phase shifts α between the elements.

to assess the exposure. Analysis of the exposure variation due to the near-field antenna/body coupling at MMW is out of the scope of this study and was presented previously [13]. For the sake of simplicity, we will refer to the equivalent source as the antenna in the paper. The total number of mesh cells reaches about 200 000 000 at 26 GHz and 300 000 000 at 60 GHz. The smallest mesh cell dimension is 46.5 µm at 26 GHz and 28.6 µm at 60 GHz, respectively. It is further reduced in the z direction at the interface between skin and air/textile, and its value is set to 2.5 µm for a total thickness of 5 µm.

III. RESULTS

The averaged absorbed power density is used as dosimetric quantity in the 6–300 GHz range [6], [7]. It is expressed as

$$PD_{av} = \frac{1}{A}\int_A \frac{1}{2}\mathrm{Re}\left[\boldsymbol{E} \times \boldsymbol{H}^*\right] \cdot d\boldsymbol{s}, \tag{2}$$

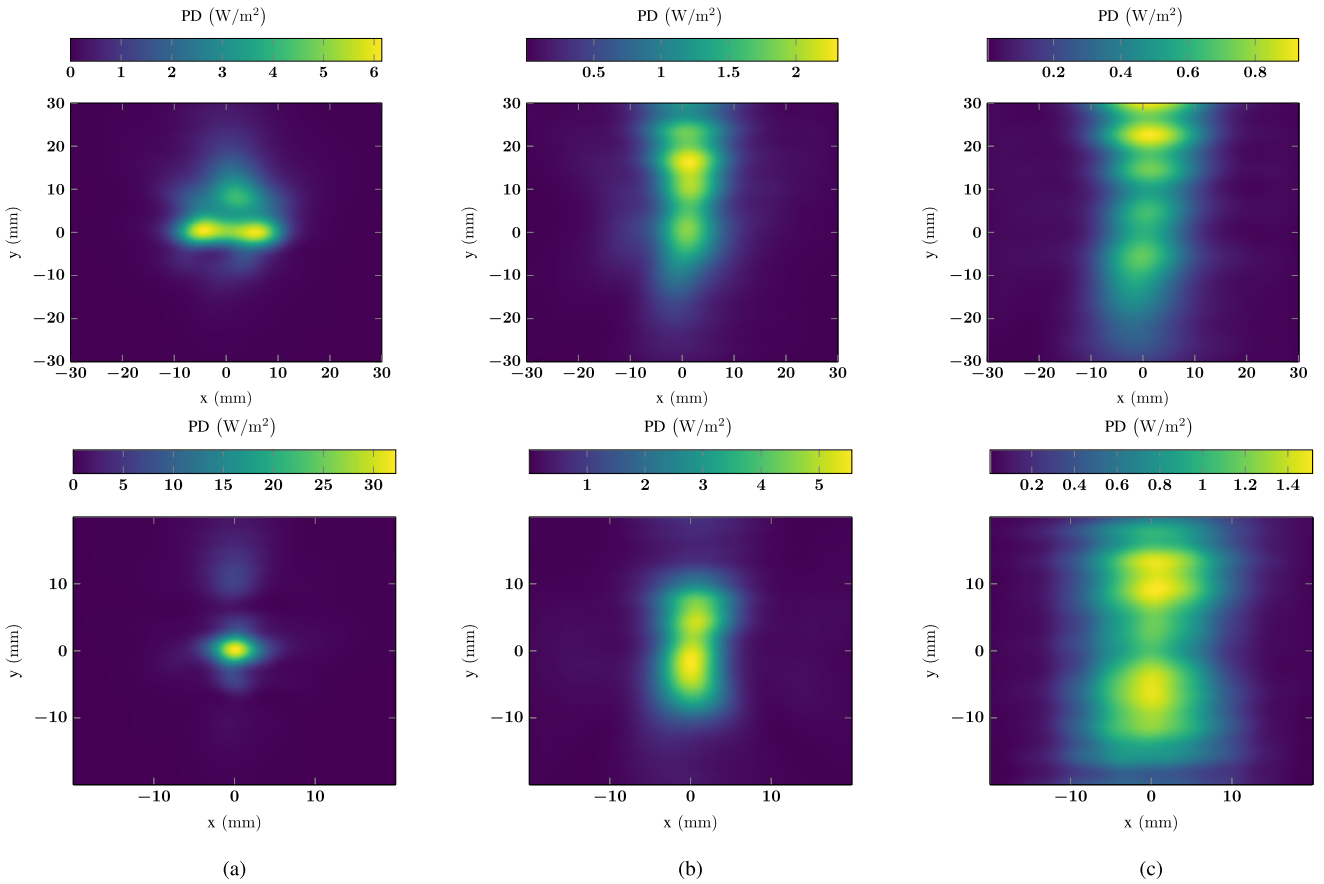

FIGURE 5. PD at 26 GHz (top) and at 60 GHz (bottom) as a function of distance d between the tissue model and antenna: (a) $d = 0.5$ cm, (b) $d = 1.5$ cm, (c) $d = 3$ cm.

where $\boldsymbol{E}$ and $\boldsymbol{H}$ are the electric and magnetic fields, respectively, A is the averaging area ($A = 4\,\text{cm}^4$ [6]) and $\boldsymbol{ds}$ is the normal to the surface. The perpendicular to the surface A component of the time averaged Poynting vector, hereafter referred to as local power density (PD), is expressed as

$$PD = \frac{1}{2}\text{Re}\left[\boldsymbol{E} \times \boldsymbol{H}^*\right] \cdot d\boldsymbol{s}\,. \tag{3}$$

Figure 5 represents the PD distribution as a function of the distance between the antenna and the skin phantom (0.5 cm, 1.5 cm, and 3 cm) when the main beam is pointing at broadside. A distance of 0.5 cm is considered as a typical spacing between the antenna and skin representing the case of a wireless device in contact with skin (e.g., smartphone during a phone call or browsing). In simulations, the antenna input power is set to 10 mW. The distributions are nearly symmetric with respect to the y axis (the origin of the coordinate system is located in the center of the bottom edge of the source box). As expected, at $d = 0.5$ cm the exposure is more localized at 60 GHz, and the peak value is higher compared to 26 GHz. The peak value decreases more rapidly with distance at 60 GHz, and at $d = 3$ cm the maximal values at the two frequencies are approaching.

Figure 6 shows the PD distribution for the antenna beam pointing at 45° from broadside when $d = 0.5$ cm. At 45°, the exposure is less localized than at 0°, and the spot produced by the exposure has almost the same extension in the y direction but is double in the x one. In addition, at 45° the antenna side lobes contribute separately from the main beam producing some additional spots in the PD distribution.

A. EFFECT OF AGEING

Figure 7 represents the variations of the PD_{av} in respect to the value for a 35 year old adult [36] for $d = 0.5$ cm. The data for Yagi antennas are compared to the plane-wave illumination [14].

For all exposure conditions, the maximum PD_{av} variations are observed for seniors and are the lowest for youth with a plateau between roughly 20 and 50 year. These variations are mainly due to the fact that the water concentration of skin decreases with age resulting in a decrease of the complex permittivity. This in turn leads to a reduction of the contrast at the skin/air interface and therefore to an increase with age of the power transmission coefficient at this interface.

At 26 GHz, for a 5 year old model the variations are −4.5% (Yagi antenna) and −2.8% (plane wave). For a 70 year old model, PD_{av} increases by 8.8% (Yagi antenna) and 6.4% (plane wave). Note that the plane-wave approximation results in an underestimation of the PD_{av} variations. At 60 GHz, the variations are almost identical for the antennas and the plane

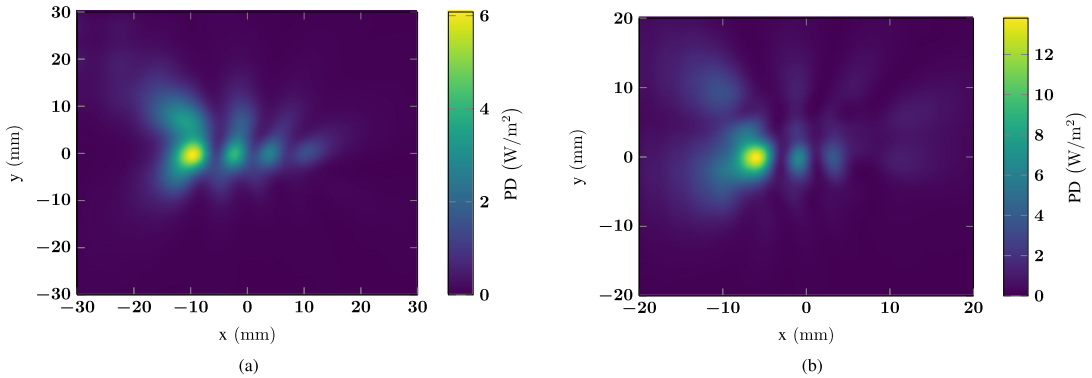

FIGURE 6. PD for $d = 0.5$cm and the beam pointing at 45° from broadside at (a) 26 GHz and (b) 60 GHz.

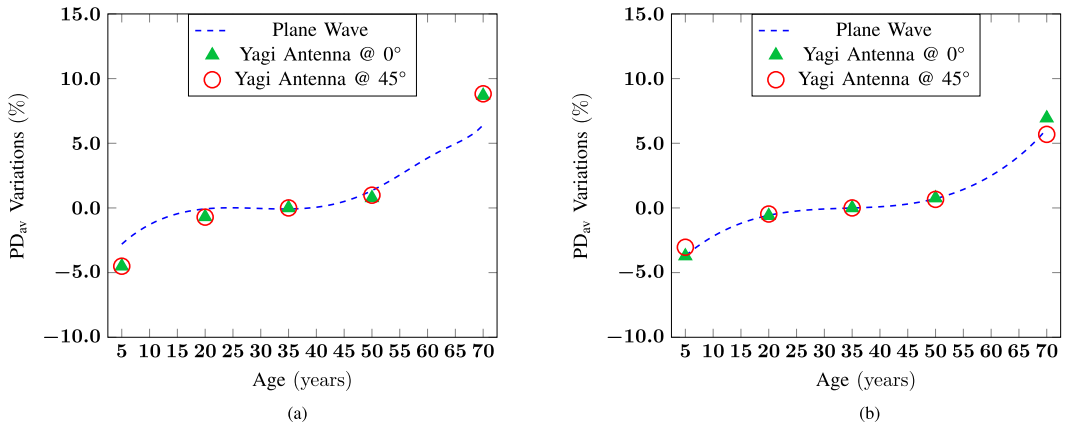

FIGURE 7. Variations of PD_{av} as a function of age with respect to the reference value at 35 year at: (a) 26 GHz, (b) 60 GHz.

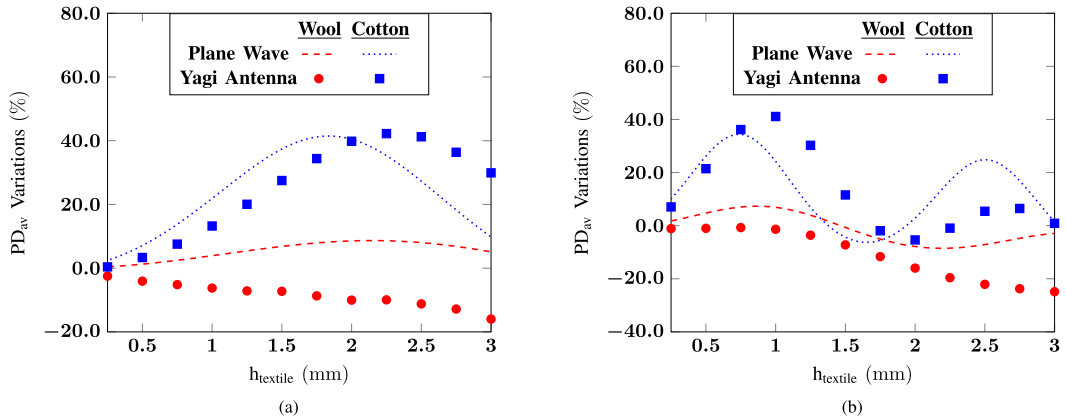

FIGURE 8. Variations of PD_{av} as a function of the textile thickness with respect to the case of bare skin, when the textile is in contact with skin at: (a) 26 GHz, (b) 60 GHz.

wave [−3% to −4% (5 year) and 5.7% to 6.9% (70 year)] Note that these PD_{av} changes are of within the typical inter-individual variations.

B. EFFECT OF CLOTHING

In contact with skin: Fig. 8 represents the variations of the PD_{av} as a function of textile thickness (h_{textile}) for the antennas pointing at broadside and at a distance of 0.5 cm. The data are compared to the results for plane wave illumination [14]. At both frequencies, presence of a textile material modifies PD_{av}. In most of the considered scenarios (Yagi antenna/wool, plane wave/cotton, plane wave/wool) PD_{av} increases with respect to the case of bare skin, except Yagi antenna/wool scenario. The order of magnitude of variations for Yagi antennas is the same as for plane wave. However, the behavior of the curves is different. For a plane wave, the highest PD_{av}

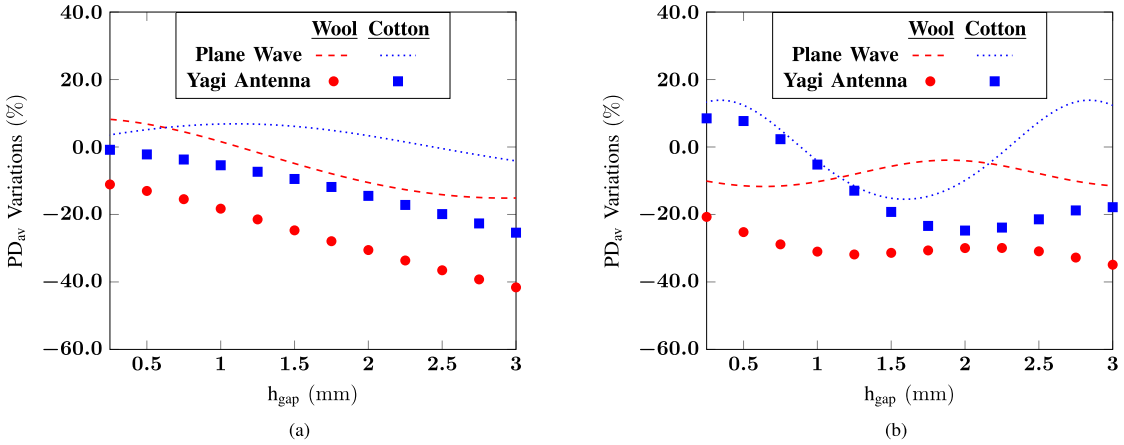

FIGURE 9. **Variations of PD$_{av}$ as a function of the thickness of an air gap between the textile and skin with respect to the case of bare skin at: (a) 26 GHz, (b) 60 GHz.**

variations are with a 1.84 mm thick cotton layer at 26 GHz (41.5%) and 0.74 mm thick at 60 GHz (34.4%). The exposure scenario with the antenna was simulated considering a textile thickness varying from 0.25 mm to 3 mm with a step of 0.25 mm. Under these conditions, the maximal variation compared to the bare skin at 26 GHz is 42.2% (2.25 mm thick cotton). At 60 GHz, the increment of the PD$_{av}$ is the highest for 1 mm thick cotton and corresponds to 41.1%.

With an air gap: To account for the presence of an air gap between the textile and skin, we added an air layer with the thickness ranging from 0.25 mm to 3 mm with a step of 0.25 mm. The antenna was placed at 0.5 mm from the textile, the main beam pointing towards broadside. The textile thickness was set to a typical value, i.e. 2 mm for wool and 0.2 mm for cotton.

Figure 9 represents the variations of the PD$_{av}$ compared to the case of bare skin for the antenna and plane wave. At 26 GHz for both textiles, PD$_{av}$ monotonically decreases with h_{gap} for Yagi antenna compared to the bare skin or textile in contact with skin ($h_{\text{gap}} = 0$ mm). Note that for the plane wave exposure, PD$_{av}$ can both increase or decrease depending on the value of h_{gap}. PD$_{av}$ reaches the maximum at 0.05 mm (+8.57%) and 1.11 mm (+6.86%) for wool and cotton, respectively. Overall, the plane wave model results in an overestimation of the PD$_{av}$ variations.

At 60 GHz, and for a 0.2-mm-thick cotton, PD$_{av}$ can exceed the value for bare skin both for plane wave and antenna source cases. For the plane wave, the highest variation of 13.87% is for $h_{\text{gap}} = 0.34$ mm or $h_{\text{gap}} = 2.84$ mm. For the antenna, the maximal increase of 8.5% occurs for $h_{\text{gap}} = 0.25$ mm. For the 2-mm-thick wool, PD$_{av}$ is lower than the one for the bare skin, and the plane wave model results in a significant overestimation of the PD$_{av}$ variations.

IV. DISCUSSION AND CONCLUSION

This study analyses the effect of ageing and textile on the power deposition in a skin-equivalent model due to near-field exposure by a representative multi-beam radiating structure at 26 GHz and 60 GHz.

The PD$_{av}$ increases with age. The highest value is observed for seniors (+8.8% at 26 GHz and +6.9% at 60 GHz with respect to the reference value at 35 year) and the lowest for youth (−4.5% at 26 GHz and −3.7% at 60 GHz) with a plateau between roughly 20 and 50 year. The plane-wave approximation results in an underestimation of the PD$_{av}$ variations at 26 GHz. At 60 GHz, the variations are almost identical for the antennas and plane wave. These variations are within the typical interindividual differences and below the safety margins used in guidelines and standards (factor of 10 for occupational exposure and 50 for general public).

When considering the presence of a textile, PD$_{av}$ can increase or decrease depending on the textile thickness and permittivity as well as on the thickness of the air gap between the textile and skin. For the two considered in this study textiles (i.e. cotton and wool), the maximum increase of the PD$_{av}$ compared to the bare skin is about 40%. The use of a plane-wave model results in an overestimation of the PD$_{av}$ variations but the order of magnitude remains the same as for near-field exposure.

Experimental validation of the numerical results would require high-resolution near-field measurements in presence of a tissue-equivalent model. Conventional methods of free-space measurement at MMW are not suited to estimate the power density on the phantom surface [42]. Use of the infrared imaging successfully employed for near-field dosimetry at MMW [43]–[45] is complicated by the presence of textiles. Adaptation of measurement techniques for validation of the numerical results constitutes one of the perspectives of this study.

REFERENCES

[1] T. S. Rappaport *et al.*, "Millimeter wave mobile communications for 5G cellular: It will work!" *IEEE Access*, vol. 1, pp. 335–349, 2013.
[2] "High five," *Nature Electron.*, vol. 3, no. 1, Jan. 2020, doi: 10.1038/s41928-020-0368-1.

[3] J. Wiart, A. Hadjem, M. F. Wong, and I. Bloch, "Analysis of RF exposure in the head tissues of children and adults," *Phys. Med. Biol.*, vol. 53, no. 13, pp. 3681–3695, Jul. 2008.

[4] J. Wang, O. Fujiwara, and S. Watanabe, "Approximation of aging effect on dielectric tissue properties for SAR assessment of mobile telephones," *IEEE Trans. Electromagn. Compat.*, vol. 48, no. 2, pp. 408–413, May 2006.

[5] E. Conil, A. Hadjem, F. Lacroux, M. F. Wong, and J. Wiart, "Variability analysis of SAR from 20 MHz to 2.4 GHz for different adult and child models using finite-difference time-domain," *Phys. Med. Biol.*, vol. 53, no. 6, pp. 1511–1525, Mar. 2008.

[6] International Commission on Non-Ionizing Radiation Protection (ICNIRP), "Guidelines for limiting exposure to electromagnetic fields (100 kHz to 300 GHz)," *Health Phys.*, vol. 118, no. 5, pp. 483–524, May 2020.

[7] *IEEE Standard for Plbibitalic-Safety Levels with Respect to Human Exposure to Electric, Magnetic, and Electromagnetic Fields, 0 Hz to 300 GHz*, IEEE Std C95.1-2019, Oct. 2019. [Online]. Available: https://ieeexplore.ieee.org/servlet/opac?punumber=8859677.

[8] J. F. Bakker, M. M. Paulides, A. Christ, N. Kuster, and G. C. van Rhoon, "Assessment of induced SAR in children exposed to electromagnetic plane waves between 10 MHz and 5.6 GHz," *Phys. Med. Biol.*, vol. 56, no. 9, pp. 2883–2883, May 2011.

[9] T. Nagaoka and S. Watanabe, "Development of voxel models adjusted to ICRP reference children and their whole-body averaged SARs for whole-body exposure to electromagnetic fields from 10 MHz to 6 GHz," *IEEE Access*, vol. 7, pp. 135909–135916, 2019.

[10] M. Heino, C. Icheln, and K. Haneda, "Finger effect on 60 GHz user device antennas," in *Proc. 10th Eur. Conf. Antennas Propag. (EuCAP)*, Davos, Switzerland, Apr. 2016, pp. 1–5.

[11] W. Hong, K.-H. Baek, and S. Ko, "Millimeter-wave 5G antennas for smartphones: Overview and experimental demonstration," *IEEE Trans. Antennas Propag.*, vol. 65, no. 12, pp. 6250–6261, Dec. 2017.

[12] A. R. Guraliuc, M. Zhadobov, R. Sauleau, L. Marnat, and L. Dussopt, "Near-field user exposure in forthcoming 5G scenarios in the 60GHz band," *IEEE Trans. Antennas Propag.*, vol. 65, no. 12, pp. 6606–6615, Dec. 2017.

[13] M. Ziane, R. Sauleau, and M. Zhadobov, "Antenna/body coupling in the near-field at 60 GHz: Impact on the absorbed power density," *Appl. Sci.*, vol. 10, no. 21, Oct. 2020, Art. no. 7392.

[14] G. Sacco, S. Pisa, and M. Zhadobov, "Age-dependence of electromagnetic power and heat deposition in near-surface tissues in emerging 5G bands," *Sci. Rep.*, vol. 11, no. 1, Feb. 2021, Art. no. 3983.

[15] O. Gandhi and A. Riazi, "Absorption of millimeter waves by human beings and its biological implications," *IEEE Trans. Microw. Theory Techn.*, vol. 34, no. 2, pp. 228–235, Feb. 1986.

[16] M. Zhadobov, N. Chahat, R. Sauleau, C. Le Quement, and Y. Le Drean, "Millimeter-wave interactions with the human body: State of knowledge and recent advances," *Int. J. Microw. Wireless Technol.*, vol. 3, no. 2, pp. 237–247, Apr. 2011.

[17] European Telecommunications Standards Institute (ETSI), "5G; NR; user equipment (UE) radio transmission and reception; Part 2: Range 2 Standalone, 3GPP TS 38.101-2 version 15.3.0 release 15," Oct. 2018. [Online]. Available: https://www.etsi.org/deliver/etsits/138100138199/13810102/15.03.0060/ts13810102v150300p.pdf

[18] European Telecommunications Standards Institute (ETSI), "Multiple-gigabit/s radio equipment operating in the 60 GHz band; harmonised standard covering the essential requirements of article 3.2 of directive 2014/53/EU, ETSI EN 302 567 V2.1.1," Jul. 2017. [Online]. Available: https://www.etsi.org/deliver/etsien/302500302599/302567/02.01.0160/en302567v020101p.pdf.

[19] S.-S. Hsu, K.-C. Wei, C.-Y. Hsu, and H. Ru-Chuang, "A 60-GHz millimeter-wave CPW-fed Yagi antenna fabricated by using 0.18-μm CMOS technology," *IEEE Electron Device Lett.*, vol. 29, no. 6, pp. 625–627, Jun. 2008.

[20] A. L. Amadjikpe, D. Choudhury, C. E. Patterson, B. Lacroix, G. E. Ponchak, and J. Papapolymerou, "Integrated 60-GHz antenna on multilayer organic package with broadside and end-fire radiation," *IEEE Trans. Microw. Theory Techn.*, vol. 61, no. 1, pp. 303–315, Jan. 2013.

[21] Y. Li and K.-M. Luk, "A multibeam end-fire magnetoelectric dipole antenna array for millimeter-wave applications," *IEEE Trans. Antennas Propag.*, vol. 64, no. 7, pp. 2894–2904, Jul. 2016.

[22] Q.-X. Chu, X.-R. Li, and M. Ye, "High-gain printed log-periodic dipole array antenna with parasitic cell for 5G communication," *IEEE Trans. Antennas Propag.*, vol. 65, no. 12, pp. 6338–6344, Dec. 2017.

[23] Y.-W. Hsu, T.-C. Huang, H.-S. Lin, and Y.-C. Lin, "Dual-polarized quasi Yagi antennas with endfire radiation for millimeter-wave MIMO terminals," *IEEE Trans. Antennas Propag.*, vol. 65, no. 12, pp. 6282–6289, Dec. 2017.

[24] W. El-Halwagy, R. Mirzavand, J. Melzer, M. Hossain, and P. Mousavi, "Investigation of wideband substrate-integrated vertically-polarized electric dipole antenna and arrays for mm-wave 5G mobile devices," *IEEE Access*, vol. 6, pp. 2145–2157, 2018.

[25] Y. Luo *et al.*, "A zero-mode induced mmWave patch antenna with low-profile, wide-bandwidth and large-angle scanning for 5G mobile terminals," *IEEE Access*, vol. 7, pp. 177607–177 615, 2019.

[26] I. M. Mohamed and A.-R. Sebak, "60 GHz 2-D scanning multibeam cavity-backed patch array fed by compact SIW beamforming network for 5G applications," *IEEE Trans. Antennas Propag.*, vol. 67, no. 4, pp. 2320–2331, Apr. 2019.

[27] M. M. Samadi Taheri, A. Abdipour, S. Zhang, and G. F. Pedersen, "Integrated millimeter-wave wideband end-fire 5G beam steerable array and low-frequency 4 G LTE antenna in mobile terminals," *IEEE Trans. Veh. Technol.*, vol. 68, no. 4, pp. 4042–4046, Apr. 2019.

[28] J. Bang and J. Choi, "A compact hemispherical beam-coverage phased array antenna unit for 5G mm-wave applications," *IEEE Access*, vol. 8, pp. 139 715–139726, 2020.

[29] J. Choi, D. Choi, J. Lee, W. Hwang, and W. Hong, "Adaptive 5G architecture for a mmWave antenna front-end package consisting of tunable matching network and surface-mount technology," *IEEE Trans. Compon. Packag. Manuf. Technol.*, vol. 10, no. 12, pp. 2037–2046, Dec. 2020.

[30] H. Li, Y. Cheng, and Z. Ling, "Design of distributed and robust millimeter-wave antennas for 5G communication terminals," *IEEE Access*, vol. 8, pp. 133 420–133 429, 2020.

[31] V. Raghavan, M.-L. Chi, M. A. Tassoudji, O. H. Koymen, and J. Li, "Antenna placement and performance tradeoffs with hand blockage in millimeter wave systems," *IEEE Trans. Commun.*, vol. 67, no. 4, pp. 3082–3096, Apr. 2019.

[32] M. F. Khajeim, G. Moradi, R. S. Shirazi, S. Zhang, and G. F. Pedersen, "Wideband vertically polarized antenna with endfire radiation for 5G mobile phone applications," *IEEE Antennas Wireless Propag. Lett.*, vol. 19, no. 11, pp. 1948–1952, Nov. 2020.

[33] C. A. Balanis, *Antenna Theory: Analysis and Design*, 3rd ed. Hoboken, NJ, USA: Wiley, 2005.

[34] Rogers Corporation, "RO4000 series high frequency circuit materials," 2018. [Online]. Available: https://rogerscorp.com/-/media/project/rogerscorp/documents/advanced-connectivity-solutions/english/data-sheets/ro4000-laminates-ro4003c-and-ro4350b---data-sheet.pdf

[35] F. S. Barnes and B. Greenebaum, "Handbook of biological effects of electromagnetic fields," *Choice Rev. Online*, vol. 33, no. 11, pp. 33–6361, Jul. 1996.

[36] C. Gabriel, "Compilation of the dielectric properties of body tissues at RF and microwave frequencies," Dept. Phys., King's College London, London, U. K., Tech. Rep. AL/OE-TR-1996-0004, Jan. 1996. [Online]. Available: https://apps.dtic.mil/dtic/tr/fulltext/u2/a303903.pdf

[37] W. C. Chumlea, S. S. Guo, C. M. Zeller, N. V. Reo, and R. M. Siervogel, "Total body water data for white adults 18 to 64 years of age: The fels longitudinal study," *Kidney Int.*, vol. 56, no. 1, pp. 244–252, Jul. 1999.

[38] J. C. K. Wells, "Prediction of total body water in infants and children," *Arch. Dis. Childhood*, vol. 90, no. 9, pp. 965–971, Sep. 2005.

[39] W. J. Ellison, "Permittivity of pure water, at standard atmospheric pressure, over the frequency range 0–25 THz and the temperature range 0–100 °C," *J. Phys. Chem. Ref. Data*, vol. 36, no. 1, pp. 1–18, Mar. 2007.

[40] P. A. Hasgall *et al.*, "IT'IS database for thermal and electromagnetic parameters of biological tissues version 4.0," May 2018. [Online]. Available: https://www.itis.swiss/virtual-population/tissue-properties/overview/

[41] A. R. Guraliuc, M. Zhadobov, G. Valerio, N. Chahat, and R. Sauleau, "Effect of textile on the propagation along the body at 60 GHz," *IEEE Trans. Antennas Propag.*, vol. 62, no. 3, pp. 1489–1494, Mar. 2014.

[42] I. Iliopoulos *et al.*, "Enhancement of penetration of millimeter waves by field focusing applied to breast cancer detection," *IEEE Trans. Biomed. Eng.*, vol. 68, no. 3, pp. 959–966, Mar. 2021.

[43] N. Chahat, M. Zhadobov, L. Le Coq, S. I. Alekseev, and R. Sauleau, "Characterization of the interactions between a 60-GHz antenna and the human body in an off-body scenario," *IEEE Trans. Antennas Propag.*, vol. 60, no. 12, pp. 5958–5965, Dec. 2012.
[44] M. Zhadobov, C. Leduc, A. Guraliuc, and R. Sauleau, "Antenna/human body interactions in the 60 GHz band: State of knowledge and recent advances," in *Advances in Body-Centric Wireless Communication: Applications and State-of-the-Art*, A. Alomainy, K. Qaraqe, M. Ur Rehman, and Q. H. Abbasi, Eds. London, U.K.: IET, Jun. 2016, pp. 97–142.
[45] C. Leduc and M. Zhadobov, "Impact of antenna topology and feeding technique on coupling with human body: Application to 60-GHz antenna arrays," *IEEE Trans. Antennas Propag.*, vol. 65, no. 12, pp. 6779–6787, Dec. 2017.

GIULIA SACCO (Member, IEEE) received the M.S. degree (*summa cum laude*) in biomedical engineering and the Ph.D. degree (*cum laude* and with the *Doctor Europaeus* label) in information and communication technology from the Sapienza University of Rome, Rome, Italy, in 2017 and 2021, respectively. She is currently a Research Fellow with the Institut d'Électronique et des Technologies du numérique, Rennes, France.

From April 2019 to September 2019, she was a Visiting Researcher with Stiching imec Eindhoven, The Netherlands. Her scientific and research interests include innovative biomedical applications of electromagnetic fields and radars for vital signs monitoring.

Dr. Sacco was the recipient of the Best Student Paper Award at Photonics and Electromagnetics Research Symposium (PIERS) 2019 and the Best Student Paper Award at the XXXIII General Assembly and Scientific Symposium (GASS) of the International Union of Radio Science (Union Radio Scientifique Internationale-URSI) 2020.

DENYS NIKOLAYEV (Member, IEEE) received the M.S. degree (*summa cum laude*) in electronics and telecommunications from Lviv Polytechnic National University, Ukraine, in 2008, and the joint Ph.D. degrees in electronics from the Institute of Electronics and Telecommunication of Rennes, Rennes, France, and in electrical engineering from the University of West Bohemia, Pilsen, Czechia, in 2017.

He was a Postdoctoral Fellow with Imec/Ghent University, Belgium, until 2018; a Scientist with École polytechnique fédérale de Lausanne, Lausanne, Switzerland, until 2020; and then joined the French National Center for Scientific Research, Paris, France, as a permanent Researcher. He has authored one book chapter, 20 journal papers, 34 publications in international conference proceedings, and holds four patents. His research interests include wireless bioelectronics and biosensors, antenna theory and design for body-centric networks, bioelectromagnetics, and numerical methods in electromagnetics.

Dr. Nikolayev was the recipient of the Best Ph.D. Dissertation Award by the Foundation Rennes One, the Young Scientist Award at the International Conference EMBEC/NBC 2017, the Best Paper Award at the URSI-France 2017 Workshop, and the Poster Award at BioEM 2015. He was a laureate of the Eiffel Excellence Doctoral Grant (2015/2016).

RONAN SAULEAU (Senior Member, IEEE) graduated in electrical engineering and radio communications from the Institut National des Sciences Appliquées, Rennes, France, in 1995, and received the Agrégation degree from the Ecole Normale Supérieure de Cachan, France, in 1996, and the doctoral degree in signal processing and telecommunications and the Habilitation á Diriger des Recherches degree from the University of Rennes 1, Rennes, France, in 1999 and 2005, respectively.

Between September 2000 and November 2005 and between December 2005 and October 2009, he was an Assistant Professor and Associate Professor with the University of Rennes 1, where, since 2009, he has been a Full Professor. He has shared the responsibility of the research activities on antennas at IETR in 2010 and 2011. He was a Co-Director of the Research Department Antenna and Microwave Devices, IETR, and Deputy Director with IETR between 2012 and 2016. He is currently the Director of IETR. He has been involved in more than 60 research projects at the national and European levels and has co-supervised 23 Postdoctoral Fellows, 44 Ph.D. students, and 50 master's students. He has received 17 patents, and is an author or coauthor of more than 250 journal papers and 510 publications in international conferences and workshops. His current research interests include numerical modeling (mainly FDTD), millimeter-wave printed and reconfigurable (MEMS) antennas, substrate integrated waveguide antennas, lens-based focusing devices, periodic and nonperiodic structures (electromagnetic bandgap materials, metamaterials, reflectarrays, and transmitarrays), and biological effects of millimeter waves.

Prof. Sauleau was the recipient of the 2004 ISAP Conference Young Researcher Scientist Fellowship, Japan, and the first Young Researcher Prize in Brittany, France, in 2001 for his research work on gain-enhanced Fabry-Perot antennas. In September 2007, he was elevated to Junior Member of the Institut Universitaire de France. He was awarded the Bronze Medal by CNRS in 2008 and the Silver Medal in 2020. He was the co-recipient of several international conference awards with some of his students (BioEM 2005, BEMS'2006, MRRS'2008, E-MRS'2011, BEMS'2011, IMS'2012, Antem'2012, BioEM'2015, and EuCAP'2019). He was the Guest Editor of the IEEE TRANSACTIONS ON ANTENNAS AND PROPAGATION Special Issue on Antennas and Propagation at mm and sub mm Waves. He was a National Delegate for several EU COST actions. He was a National Delegate for EurAAP and a Member on the Board of Director of EurAAP from 2013 to 2018.

MAXIM ZHADOBOV (Senior Member, IEEE) received the M.S. degree in electromagnetics from the University of Nizhny Novgorod, Nizhny Novgorod, Russia, in 2003, and the Ph.D. and Habilitation á Diriger des Recherches degrees from the Institut d'Electronique et des Technologies du numerique (IETR), University of Rennes 1, Rennes, France, in 2006 and 2016, respectively.

He was a Postdoctoral Researcher with the Center for Biomedical Physics, Temple University, Philadelphia, PA, USA, until 2008, and then joined the French National Center for Scientific Research (CNRS).

He is currently the Principal Investigator of biomedical electromagnetics with the IETR/CNRS and the Head of the WAVES Research Team, IETR. He has coauthored five book chapters, five patents, more than 75 research papers in peer-reviewed international journals, and 180 contributions to conferences and workshops. His research interests include innovative biomedical applications of electromagnetic fields and associated technologies. His review article in the *International Journal of Microwave and Wireless Technologies* was the most cited paper in 2016–2020. A paper published by his research group in 2019 is in journal Top 100 of Nature Scientific Reports. He has been involved in 24 research projects (12 as PI).

Dr. Zhadobov was the TPC Co-Chair of BioEM 2021 and BioEM 2020. He was a TPC Member and/or Session Organizer at international conferences, including BioEM 2019, EuMW 2019, IEEE iWEM 2017, MobiHealth 2015–2017, BodyNets 2016, and IMWS-Bio 2014. He is an elected Member of EBEA Council, Member of IEEE TC95.4, and Vice-President of URSI France Commission K. He was the Guest Editor of several special issues, including Human Exposure in 5 G and 6 G Scenarios of Applied Sciences and Advanced Electromagnetic Biosensors for Medical, Environmental and Industrial Applications of Sensors. He was also on review boards of more than 15 international journals and conferences, and has been acting as an expert at research councils worldwide. He was the recipient of the CNRS Medal in 2018, the EBEA Award for Excellence in Bioelectromagnetics in 2015, and Brittany's Young Scientist Award in 2010. Since 2010, his Ph.D. students have been recipients of seven national scientific awards and five awards from the Bioelectromagnetics Society, URSI, and the IEEE Antennas and Propagation Society.